Griseofulvin Radiosensitizes Non–Small Cell Lung Cancer Cells and Activates cGAS

Xing Wang[1,2], Natasha Raman[1], Ghali Lemtiri-Chlieh[1], Jinhee Chang[1,3], Shreya Jagtap[1,3], Dipanwita Dutta Chowdhury[1,3], Matthew Ballew[1], Francesca Anna Carrieri[1,3], Triet Nguyen[1,3], Katriana Nugent[1], Travis Peck[1], Michelle S. Levine[4], Aaron Chan[3], Christine Lam[1], Reem Malek[1], Tung Hoang[1], Ryan Phillips[1,5], ZhuoAn Cheng[1,6], Kekoa Taparra[1,7], Nick Connis[8], Christine L. Hann[8], Andrew Holland[4,8], Phuoc T. Tran[1,3,8,9], Audrey Lafargue[1,3], and Hailun Wang[1,10]

ABSTRACT

Extra copies of centrosomes are frequently observed in cancer cells. To survive and proliferate, cancer cells have developed strategies to cluster extra-centrosomes to form bipolar mitotic spindles. The aim of this study was to investigate whether centrosome clustering (CC) inhibition (CCi) would preferentially radiosensitize non–small cell lung cancer (NSCLC). Griseofulvin (GF; FDA-approved treatment) inhibits CC, and combined with radiation treatment (RT), resulted in a significant increase in the number of NSCLC cells with multipolar spindles, and decreased cell viability and colony formation ability *in vitro*. *In vivo*, GF treatment was well tolerated by mice, and the combined therapy of GF and radiation treatment resulted in a significant tumor growth delay. Both GF and radiation treatment also induced the generation of micronuclei (MN) *in vitro* and *in vivo* and activated cyclic GMP-AMP synthase (cGAS) in NSCLC cells. A significant increase in downstream cGAS-STING pathway activation was seen after combination treatment in A549 radioresistant cells that was dependent on cGAS. In conclusion, GF increased radiation treatment efficacy in lung cancer preclinical models *in vitro* and *in vivo*. This effect may be associated with the generation of MN and the activation of cGAS. These data suggest that the combination therapy of CCi, radiation treatment, and immunotherapy could be a promising strategy to treat NSCLC.

Introduction

Lung cancer is the most common cause of cancer mortality in the United States and across the world (1, 2). Non–small cell lung cancer (NSCLC) accounts for 80% of lung cancers and patients with unresectable stage III NSCLC comprise approximately 40% of all lung cancers. The standard treatment, with concurrent platinum-based chemoradiation and adjuvant immune checkpoint blockade, is not curative in the majority of patients in part due to radioresistance of the primary tumor (3, 4). In particular, patients presenting with an oncogenic mutation in the *KRAS* gene—about one-quarter of patients with NSCLC—remain recalcitrant to current therapeutic options. This finding reveals an urgent need to identify novel molecular targets to increase lung cancer radiosensitivity and increase antitumor immune systemic effects.

Centrosomes are cytoplasmic organelles composed of a pair of centrioles, which nucleate and anchor microtubules (MTs). During mitosis, normal cells possess two centrosomes each migrating to opposite poles of the cell to form a bipolar mitotic spindle. Interestingly, in contrast to normal cells, cancer cells frequently contain extra-centrosomes that can be generated during the course of tumorigenesis or induced by treatments like radiotherapy (5, 6). The presence of supernumerary centrosomes often leads to multipolar mitotic spindle formation and subsequent stress and inviable mitotic division. Cancer cells have developed strategies to cluster supernumerary centrosomes into two functional spindle poles (pseudobipolar) enabling tumor cells to divide and survive. Therefore, preventing centrosome clustering (CC) provides a means to selectively kill cancer cells with extra-centrosomes by forcing them into detrimental multipolar divisions without affecting the divisions of normal cells with normal numbers of centrosomes (7). Griseofulvin (GF), an orally active antifungal drug in humans, has attracted considerable interest as a potential anticancer agent owing to its low toxicity and efficiency in inhibiting the proliferation of different types of cancer cells (8–12). Recently, it has been shown that GF induced multipolar spindle formation in tumor cells with supernumerary centrosomes and resulted in cell death (9, 11, 13, 14). Furthermore, GF treatment arrested tumor cells at the G_2–M-phase of cell cycle and inhibited progression at metaphase and anaphase of mitosis (9, 11, 13, 14). Cancer cells are most sensitive to radiation in the G_2–M-phase of the cell cycle (15–17). Thus, CC inhibition (CCi) could result in the selective

[1]Department of Radiation Oncology and Molecular Radiation Sciences, Johns Hopkins University, School of Medicine, Baltimore, Maryland. [2]Department of Breast and Thyroid Surgery, Second Affiliated Hospital of Chongqing Medical University, Chongqing, P.R. China. [3]Department of Radiation Oncology, Division of Translational Radiation Sciences, University of Maryland Baltimore, School of Medicine, Baltimore, Maryland. [4]Department of Molecular Biology and Genetics, Johns Hopkins University, School of Medicine, Baltimore, Maryland. [5]Department of Radiation Oncology, The Mayo Clinic, Rochester, Minnesota. [6]State Key Laboratory of Oncogenes and Related Genes, Renji Hospital, School of Biomedical Engineering, Shanghai Jiao Tong University, Shanghai, P.R. China. [7]Department of Radiation Oncology, Stanford Medicine, Stanford, California. [8]Department of Oncology, Sidney Kimmel Comprehensive Cancer Center, Johns Hopkins University, School of Medicine, Baltimore, Maryland. [9]Department of Urology, James Buchanan Urological Institute, Johns Hopkins University, School of Medicine, Baltimore, Maryland. [10]GenoImmune Therapeutics, Wuhan, P.R. China.

X. Wang, N. Raman, and G. Lemtiri-Chlieh contributed as co-first authors.

A. Lafargue and H. Wang as co-corresponding senior authors to this article.

Corresponding Authors: Audrey Lafargue, University of Maryland Baltimore, School of Medicine, 655 West Baltimore St, Bressler Research Building, Rm 8-020, Baltimore, MD 21201. Phone: 410-706-1339; E-mail: alafargue@som.umaryland.edu; and Hailun Wang, GenoImmune Therapeutics, 388 Gaoxin 2nd Rd., Donghu New District, Wuhan, China. E-mail: wanghailun@hotmail.com

Mol Cancer Ther 2023;22:519–28

doi: 10.1158/1535-7163.MCT-22-0191

radiosensitization of cancer cells with supernumerary centrosomes by reducing clonogenic potential while sparing healthy tissues with normal centrosome numbers.

In this study, we investigated the effect of GF-induced CCi on radiation treatment of NSCLC *in vitro* and *in vivo*. Our results showed that CCi forced the formation of multipolar spindles in NSCLC cell lines but not in normal cells (immortalized human bronchial epithelial cells, HBECs). CCi decreased cell viability and inhibited the proliferation of NSCLC cells *in vitro*. The combination of CCi and radiation treatment significantly sensitized NSCLC cells to radiation treatment. *In vivo*, GF treatment was well tolerated, and the combination therapy of GF and radiation treatment sensitized tumors, compared with radiation treatment alone, resulting in a significant tumor growth delay. Interestingly, GF treatment induced the generation of micronuclei (MN) and promoted the translocation of cyclic GMP-AMP (cGAMP) synthase (cGAS) into these MN, with the most significant increase seen after combined treatment of GF and radiation. MN formation has been previously shown to activate the cytoplasmic double-stranded DNA sensor pathway cGAS, which in turn activates an innate immune response (18). We show that GF treatment activated the cGAS-STING pathway and increased gene expression of the downstream cytokine *CCL5* in multiple NSCLC cell lines. Interestingly, the level of *CCL5* increased the most with combined radiation treatment and GF treatment in the radioresistant cell line A549, and this *CCL5* upregulation (as well as *ISG15* and *TNF-alpha*) was dependent on cGAS.

Materials and Methods

Cell culture, antibodies, and reagents

Human *KRAS*-mutant lung cancer cell lines [H460 (CVCL_0459), H358 (CVCL_1559), and A549 (CVCL_0023)] were purchased from ATCC. The immortalized normal HBEC (CVCL_X491) line was a gift from Dr. Stephen Baylin. All cancer cell lines were authenticated by short tandem repeat profiling at the Genetic Resources Core Facility at the Johns Hopkins University (JHU, Baltimore, MD). Cells were tested (Genetic Resources Core Facility - JHU) and treated when found positive with plasmocin (InvivoGen) routinely to avoid *Mycoplasma* contamination. Cell culture methods and the antibodies used are listed in Supplementary Materials and Methods. GF (Sigma-Aldrich, G4753), Herring testis double-stranded DNA (HTdsDNA; Sigma, D6898), Polyoxyl-35 castor oil (Sigma-Aldrich, C5135), and Trypan blue solution (T8154, Sigma) were purchased from Sigma-Aldrich. For caspase-3 and cleaved caspase-3 assays, cells were harvested after incubation with GF (30 μmol/L) after 48 hours. For cGAS assays, cells were harvested after treatment with GF and irradiation after 48 hours.

Cell viability assay

Cell viability was determined at indicated timepoints based on the Trypan blue exclusion method as described previously (19). A total of 3×10^4 cells were seeded into each well of the 6-well plates. The numbers of viable cells were manually counted daily.

Radiation treatment

In vitro, cells were irradiated with 0 to 8 Gy at room temperature using the CIXD Biological X-rays Irradiator (Xstrahl; SKCCC Experimental Irradiators Core - JHU) or the X-RAD320 irradiator (Precision X-ray - University of Maryland Baltimore-DTRS). For *in vivo* experiments, mice were treated with X-rays using the Small Animal Radiation Research Platform (Xstrahl; SKCCC Experimental Irradiators Core - JHU; refs. 20, 21). Hind flank tumors received 2×2 Gy irradiation daily using a circular 1-cm diameter beam.

Clonogenic assay

The procedure (22) was described in the Supplementary Materials and Methods.

Immunoblot analysis

The Western blot procedure was described in the Supplementary Materials and Methods.

Immunofluorescence staining

Immunofluorescence (IF) was performed as described previously (ref. 23; Supplementary Materials and Methods).

Spindle polar detection

All nuclei were detected and segmented using DAPI staining (total cell number). Mitotic spindle formation was confirmed by α-tubulin staining. Pericentrin staining was used to identify centrosomes. Bipolar spindles present with one centrosome per pole (two centrosomes per cell). Mitotic cells with greater than two division poles were classified as multipolar spindles. Centrosome clustering was defined by the presence of a pseudobipolar spindle associated with more than one centrosome per pole.

IHC

IHC was described in the Supplementary Materials and Methods (23).

Assessment of micronucleus and cGAS-positive MN frequency

In vitro, the percentage of cells with MN was determined by microscopy under blinded conditions. Micronucleated cells were classified manually by distinct staining by DAPI of structures outside of the main nucleus. Cells with an apoptotic appearance were excluded. For *in vivo* micronucleus assay, hematoxylin and eosin (H&E) staining procedures were performed by the JHU Tissue Core Facility. Slides were observed under a Nikon Eclipse Ni microscope equipped with a Nikon digital site DS-U3 camera under 40X magnification. All MN grading was performed in a double-blinded fashion. At least 500 cells per core were counted. The criteria for the MN included (i) the same staining as the main nucleus, (ii) smaller than the diameter of the main nucleus, and (iii) not attached to the main nucleus. To enumerate cGAS-positive MN, these structures were counted manually for each field and expressed as a percentage of total cells within the field. Total cells were counted manually based on the DAPI and cGAS. More than 500 cells were quantified for each sample.

Xenograft mouse model

Mice were purchased from Harlan Laboratories and housed and maintained in accordance with the guidelines from our Institutional Animal Care and Use Committee (IACUC) at the JHU School of Medicine (approved protocol No. MO18M195/MO21M205). Female and male nude (NCRNU, sp/sp) mice 4 to 5 weeks old (eight subjects per condition) were injected subcutaneously in the flanks with 1×10^6 H358 cells in 100 μL of Hank's solution and Matrigel (BD Biosciences) mixed 1:1. Once tumors reached 100 mm^3, mice were treated or not with GF (50 mg/kg) and/or radiation treatment (2 Gy × 2). GF was dissolved in 100% DMSO first and then diluted with 10% castor oil (final 9% DMSO). The mice received vehicle or GF daily (5 days a week) via intraperitoneal injections (11). Three days after starting GF treatment, mice were irradiated. After 3 days of irradiation, two of the mice in each group were sacrificed, and the tumors were assessed by H&E, Ki67, and cleaved caspase-3 staining. After 21 days of treatment, all mice were sacrificed. The tumor volume [(length × $width^2$)/2] and

animal weight were measured every 2 to 4 days. Tumor growth curve was developed on the basis of the tumor size. Tumor weight was measured after mice were sacrificed.

qRT-PCR and siRNA

The primers, siRNAs, and reagents were detailed in Supplementary Materials and Methods.

Statistical analysis

All *in vitro* experiments were repeated at least three times. All *in vivo* experiments were using groups of eight mice per arm. Data were analyzed by Student *t* test or one-way ANOVA. A P value < 0.05 was considered statistically significant. All statistical analyses and graphs were carried out by using Graphpad Prism v8.4.3 (GraphPad Software; SCR_002798).

Study approval

All animal experiments were performed in accordance with the Johns Hopkins IACUC protocols (approved protocol No. MO18M195/MO21M205). Animals were housed in a pathogen-free environment in the animal facility of the JHU School of Medicine, SKCCC, Cancer Research Building.

Data availability statement

The data generated in this study are available within the article and its Supplementary Data.

Results

CCi induced multipolar spindle formation in NSCLC cells

Mammalian somatic cells typically possess one centrosome, which is duplicated in coordination with DNA replication. Each centrosome then migrates to a cell pole during cell division, forming a bipolar spindle to ensure symmetric chromosome segregation. The number of centrosomes in cancer cells can be quite heterogeneous, even within the same cell population. Hence, a cancer cell population can contain a mix of bipolar spindles, multipolar spindles with asymmetric division, and pseudobipolar spindles with CC as a prosurvival mechanism. NSCLC tumor tissues and cancer cell lines contain various levels of centrosome amplification (CA) across the entire population, and levels can range from ±5% to ±40% depending on the cell line (24–26). To examine the effect of CC-inhibiting drug GF on *KRAS*-mutated NSCLC cells and normal cells, three *KRAS*-mutated NSCLC cell lines, A549, H358, and H460, and one non-cancer cell line, HBEC, were used. The basal levels of CA were heterogeneous within

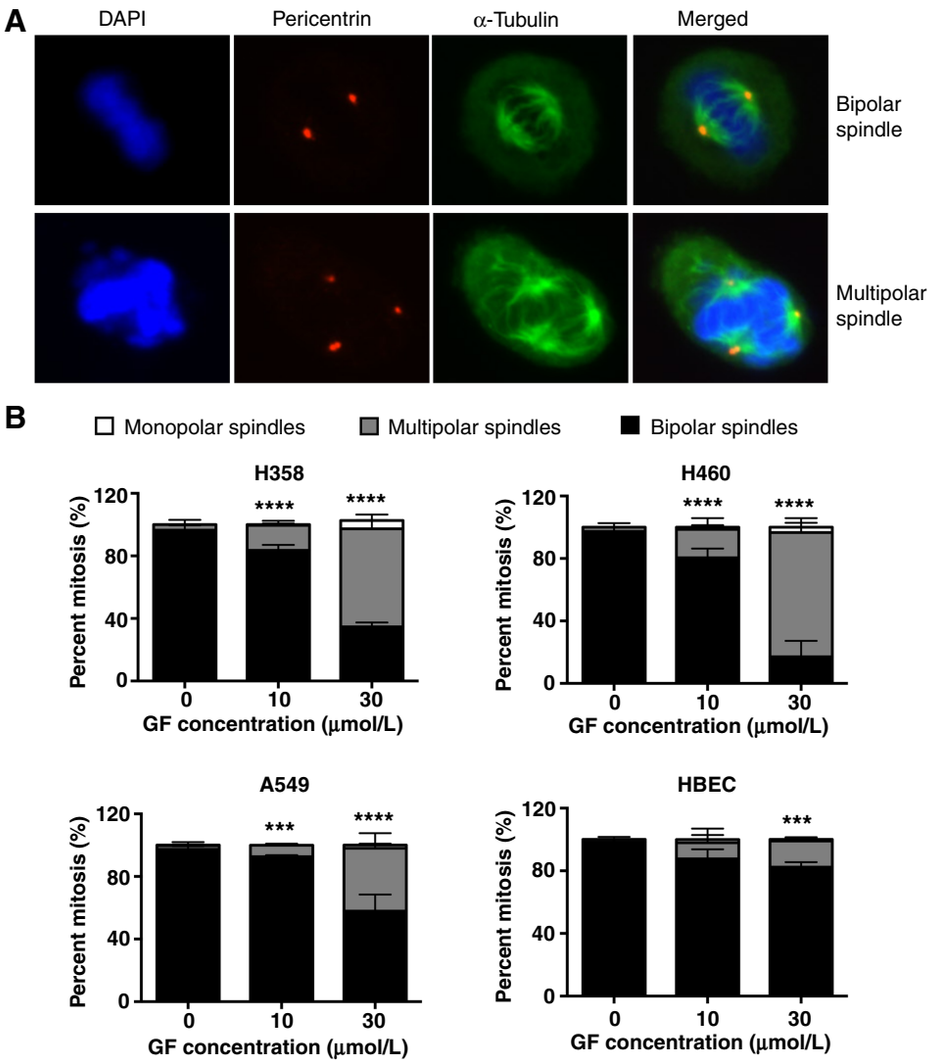

Figure 1.
CCi induced multipolar spindle formation in NSCLC cells. **A,** Representative images showing mitosis with amplified centrosomes. Cells were immunostained with α-tubulin (MTs, green), pericentrin (centrosomes, red), and DAPI (DNA, blue). **B,** The proportions of monopolar spindles, bipolar spindles, and multipolar spindles in the control and GF-treated cells were statistically analyzed. Data were shown as average value ± SD calculated from three independent experiments (one-way ANOVA; ***, $P < 0.001$; ****, $P < 0.0001$).

each population, and the average frequency of CA (percentage of cells with >2 centrosomes over the total number of cells) was <1% in HBECs and higher, ±10%, in NSCLC cells (Supplementary Fig. S1A). Then, mitotic cells were characterized as monopolar spindle, bipolar spindle, or multipolar spindle by immunostaining with anti-α-tubulin and anti-pericentrin (**Fig. 1A**). GF significantly reduced the mitotic cells with bipolar spindles and increased the ratio of multipolar spindles in all cell lines at the highest dose tested of 30 μmol/L. However, GF caused significantly more multipolar spindles in NSCLC cells than in HBEC, (40%–80% in NSCLC cells vs. 17% in HBEC with 30 μmol/L GF treatment; **Fig. 1B**). These results demonstrate that GF preferentially induced multipolar spindles in NSCLC cells over normal cells.

CCi reduced cell viability and could induce apoptotic cell death

GF treatments resulted in a time- and dose-dependent inhibition in cell growth of NSCLC and HBECs (Supplementary Fig. S2A). GF 10 μmol/L treatment significantly inhibited cell proliferation in NSCLC cells, but only slightly slowed the proliferation of HBECs. Higher concentrations of GF (30 μmol/L) severely inhibited growth of all cell lines (Supplementary Fig. S2A). Trypan blue exclusion assay showed that the percentage of dead cells was significantly higher in H358 and H460 cells after GF treatment compared with that in A549 and HBEC (Supplementary Fig. S2B). After a genotoxic or MT-toxic stress, plural cell responses concomitantly exist within the cell population including mitotic catastrophe but also apoptosis, the induction of a senescent or an arrested phenotype. We also observed an induction of cleaved caspase-3 in H358 and H460 with GF treatment consistent with the induction of cell death (Supplementary Fig. S2C). The fact that we do not observe a cleaved caspase-3 induction for A549 might suggest an induction of a senescent or arrested phenotype, or possibly also mitotic catastrophe that could lead to a loss of these cells from the overall population at the timepoint of analysis.

GF reduced centrosome clustering in NSCLC cells after radiation treatment

Irradiation can induce CA in cancer cells, and clustering these extra-centrosomes is a strategy for cancer cells to avoid multipolar mitoses. We examined CC events in NSCLC cells after radiation

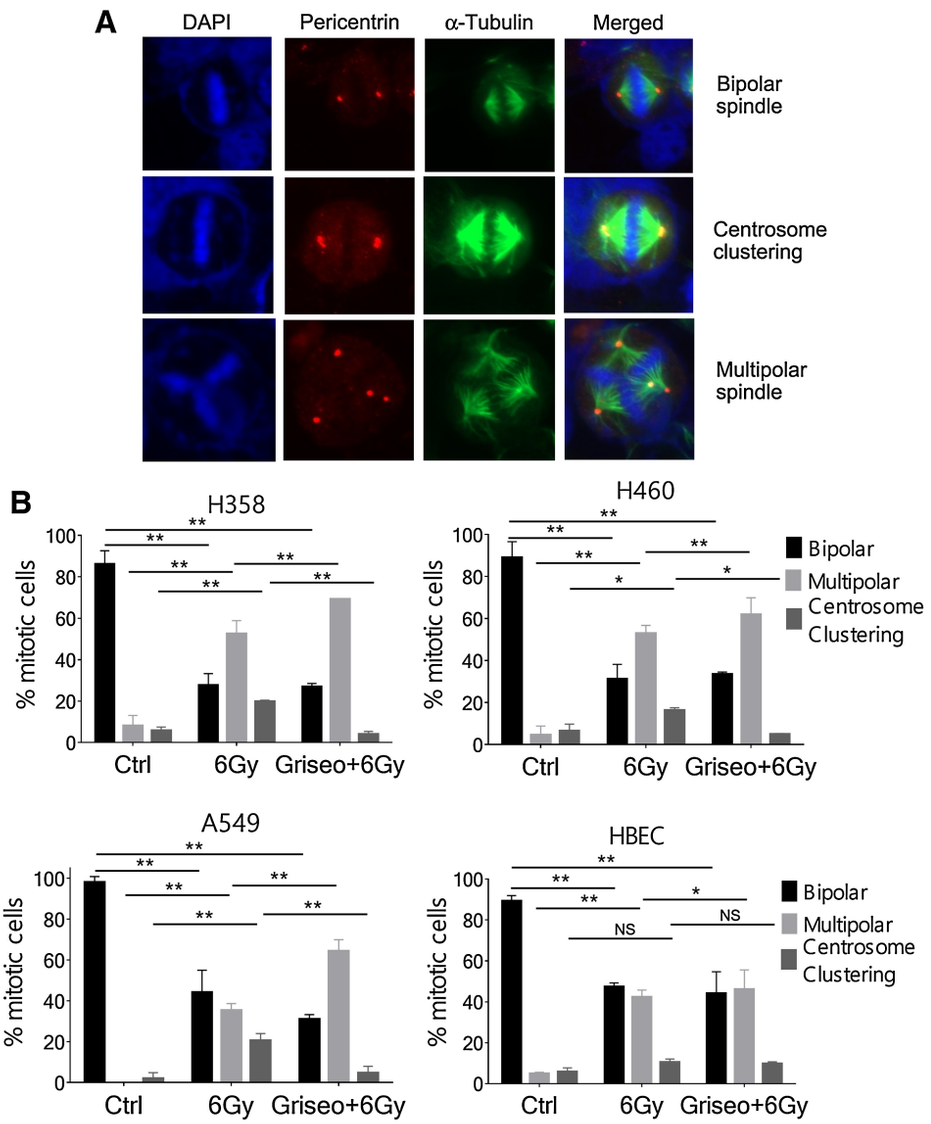

Figure 2.

GF reduced centrosome clustering in NSCLC cells after radiation treatment. **A,** Representative images showing mitosis with normal bipolar, clustered supernumerary centrosomes and multipolar spindles. Cells were immunostained with α-tubulin (MTs, green), pericentrin (centrosomes, red), and DAPI (DNA, blue). **B,** Quantification of the percentage of normal bipolar spindles, centrosome-clustering bipolar spindles, and multipolar spindles. Data were shown as average value ± SD calculated from three independent experiments (one-way ANOVA; *, $P < 0.05$; **, $P < 0.01$; NS, not significant).

treatment. CC was identified via the presence of pseudobipolar spindles involving more than one centrosome per pole (**Fig. 2A**). As expected, the number of mitotic cells with multipolar spindles was significantly increased after radiation treatment (0%–5% in control vs. 36%–53% after radiation treatment; **Fig. 2A** and **B**). The number of mitotic cells with CC was also increased after radiation treatment (2%–6% in control to 16%–21% in NSCLC cells that received radiation treatment). GF treatment significantly reduced the number of mitotic cells with clustered centrosomes from 16–21% after radiation treatment alone to 4–5% in RT+GF-treated NSCLC cells, and further increased the ratio of cells with multipolar spindles (36%–53% in radiation treatment alone to 63%–69% in NSCLC cells that received radiation treatment and Griseofulvin). CC was observed less in HBEC cells (10%) after radiation treatment and there was no difference following GF treatment (**Fig. 2A** and **B**).

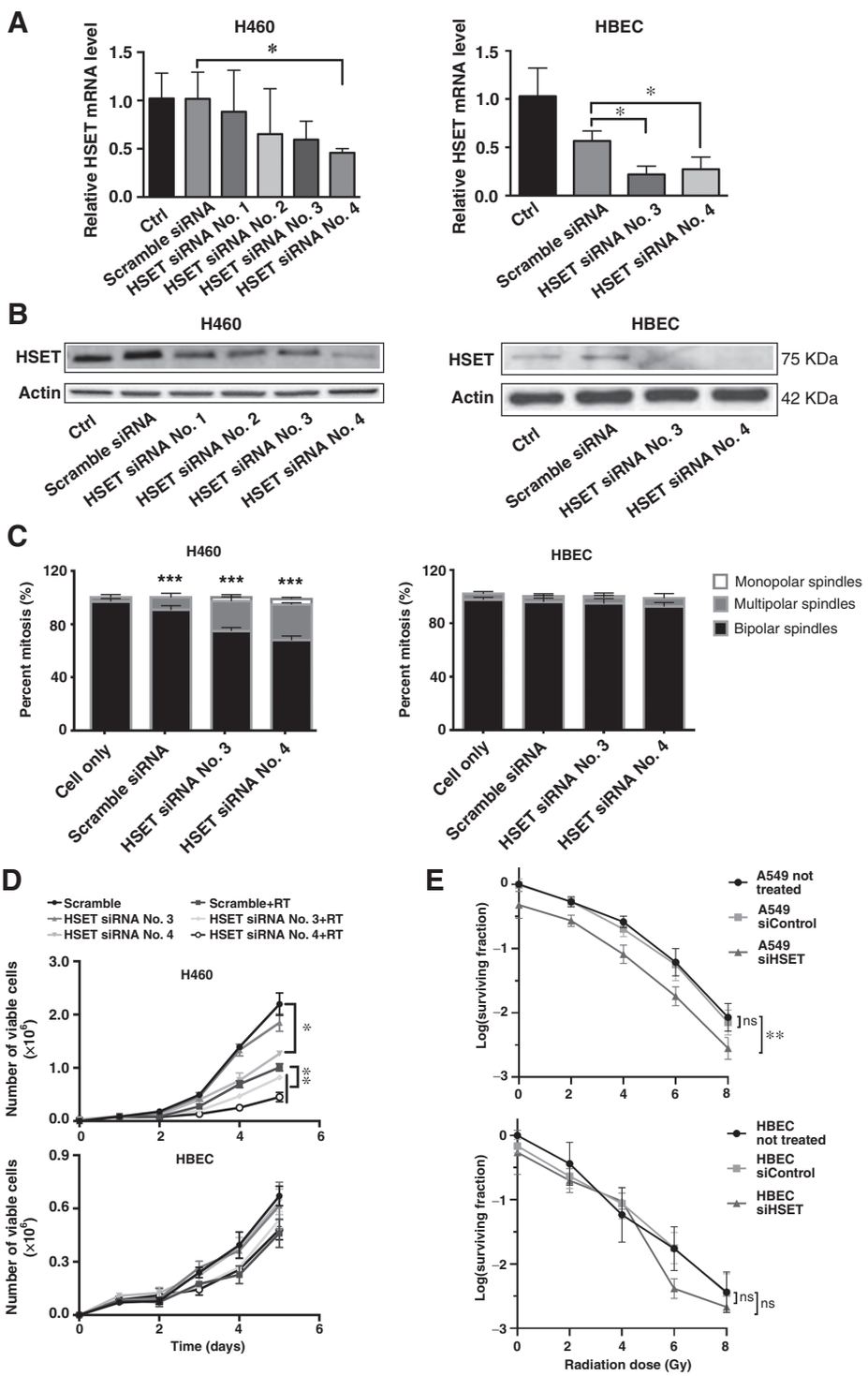

Figure 3.

Genetically targeting centrosome clustering by knocking down HSET reduced NSCLC cell viability after radiation treatment. qPCR of *HSET* gene expression (**A**) and Western blot (**B**) of HSET protein levels after knocking down *HSET* with siRNAs in H460 and HBECs. **C,** Quantification of monopolar, bipolar, and multipolar spindles after HSET knockdown. **D,** Cell proliferation of H460 and HBEC after combined HSET knockdown and radiation treatment (RT). **E,** Clonogenic survival curves for A549 and HBEC treated with or without *HSET* siRNA 48 hours before irradiation. Data were shown as average value ± SD calculated from three independent experiments (*t* test/one-way ANOVA; ns, $P > 0.05$; *, $P < 0.05$; **, $P < 0.01$; ***, $P < 0.001$).

Targeting centrosome clustering reduced NSCLC cell viability following irradiation

Next, we studied whether CCi could potentially radiosensitize tumor cells. The HSET protein, a key regulator of CC in cancer cells (7), was knocked down with siRNAs in H460 and HBEC (**Fig. 3A** and **B**). Interestingly, HSET levels were significantly higher in cancer cells than in HBEC (Supplementary Fig. S3). Consistent with other reports, reduced levels of HSET resulted in a significant increase in the number of cells with multipolar spindles in H460, but not in HBECs (**Fig. 3C**). When we treated these cells with radiation treatment, knockdown of HSET significantly reduced H460 cell viability after radiation treatment, but not HBEC (**Fig. 3D**). The knockdown of HSET also significantly reduced the clonogenic potential and radiation response of A549 cells but not of HBEC (**Fig. 3E**). Therefore, genetically targeting CC showed preferential effects on radiation-induced cell viability and clonogenic potential in NSCLC cells over noncancer cells. Similarly, pharmacologic CCi with GF significantly enhanced the radiation sensitivity in H358 and H460 cells, but not in HBECs (Supplementary Fig. S4).

GF treatment radiosensitized NSCLC in a xenograft mouse model

We also examined the radiosensitization effect of GF in a H358 xenograft mouse model. Mice bearing H358 flank tumors were treated with either GF, radiation treatment, or both. GF or radiation

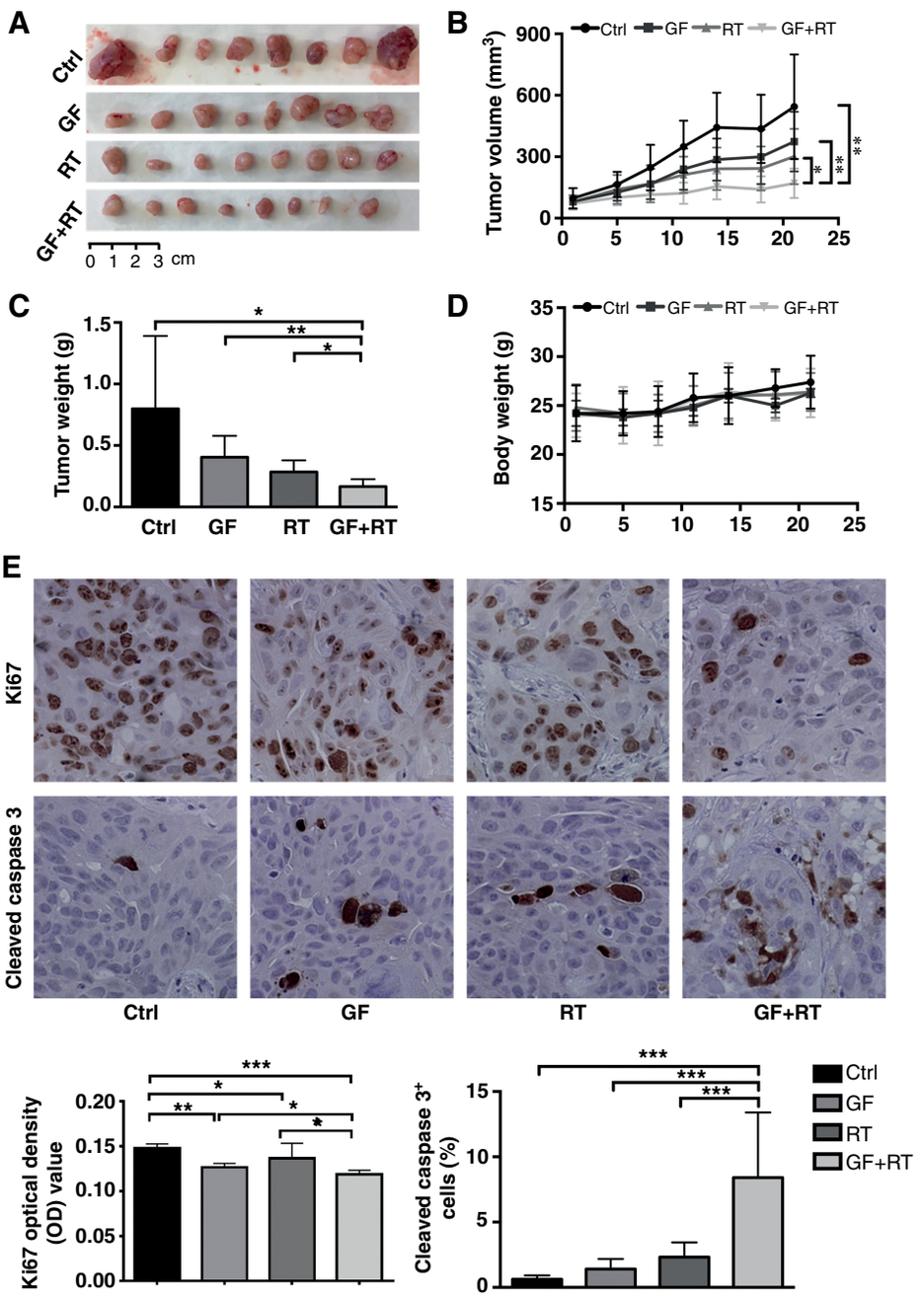

Figure 4.

GF treatment radiosensitized H358 NSCLC *in vivo*. **A,** Representative images showing the tumor sizes from each treatment group. **B,** Plots of tumor growth curves. **C,** Weight of the tumors from each treatment group. **D,** Plots of body weights of tumor-bearing mice from day 0 to day 21. **E,** Representative images of immunostaining of Ki67 and cleaved caspase-3 and quantification of positive stained cells in Ctrl, GF, RT, and GF+RT tumors. Data were shown as average value ± SD calculated from three independent experiments (one-way ANOVA; *, $P < 0.05$; **, $P < 0.01$; ***, $P < 0.001$). RT, radiation treatment.

treatment alone slowed tumor growth, but the combination of GF and radiation treatment showed further inhibition of tumor growth (**Fig. 4A–C**). GF treatment appeared well tolerated on the mice as determined by weight loss (**Fig. 4D**). We also collected tumor tissues after 3 days of irradiation and stained with Ki67 for proliferating tumor cells and cleaved caspase-3 for apoptotic cells. Consistent with the tumor growth delay results, less Ki67-positive cells were observed in GF alone or radiation treatment groups compared with the control group. The lowest number of Ki67-positive cells was observed in the combination treatment group (**Fig. 4E**). Similarly, the combination treatment resulted in the highest ratio of apoptotic cells in the tumors (**Fig. 4E**). Overall, these results demonstrated that the combination of GF and radiation treatment significantly inhibited tumor growth *in vivo* compared with single-treatment arms.

GF treatment generated MN and activated cGAS

Multipolar mitosis frequently results in MN formation (27), as does radiation treatment alone (28). We observed that GF or radiation treatment alone induced MN generation in both NSCLC cell lines *in vitro* and xenograft tumor tissues *in vivo* (**Fig. 5A**; Supplementary Fig. S5A). Interestingly, the combination treatment of GF + radiation treatment produced the most MN *in vitro* and *in vivo* (**Fig. 5A**; Supplementary S5A). Generation of MN can activate the cytoplasmic double-stranded DNA sensor pathway cGAS-STING, which can trigger an innate immune response (29). We then observed that more MN were stained positively with cGAS after combination treatment than with either single treatment in all three NSCLC cell lines *in vitro* (**Fig. 5B** and **C**; Supplementary S5B). However, no cGAS-positive MN were observed in similarly treated HBECs. The activation of the cGAS-STING pathway includes the activation of downstream factors (e.g., TBK1, NFκB, IRF3), which cooperate together to induce the transcription of multiple target genes, including IFNs and cytokines (e.g., CCL5, ISG15, IFN-β, TNF-α). We observed that the expression of STING and the phosphorylation of TBK1 were slightly upregulated after 6 Gy irradiation alone or after GF + 6 Gy combined treatment and that the combined treatment also enhanced the phosphorylation of NFκB compared with single treatment (**Fig. 6A**). We then analyzed the main downstream target genes of the cGAS signaling in NSCLC cells after the different treatments. We found that GF and radiation single treatments significantly induced the expression of *CCL5* cytokine in A549 and H460 (**Fig. 6B**). The combination GF+radiation treatment further increased *CCL5* levels in A549 cells (**Fig. 6B**). A similar profile in A549 was observed for additional cGAS pathway downstream transcriptional targets including *IFN-β-1*, *ISG15*, and *TNF-α* (**Fig. 6C** and **D**; Supplementary Fig. S6). Finally, the knockdown of cGAS in A549 and HBEC using siRNA against cGAS (smartpool siRNA cGAS) showed that the upregulation of these transcriptional targets (*CCL5*, *ISG15*, and *TNF-α*) were cGAS dependent in A549 (**Fig. 6C** and **D**). HBEC had low levels of cGAS and as expected showed little change with or without treatment regardless of knockdown (**Fig. 6C**). Altogether, we show that GF inhibits CC and results in MN formation and activation of the cGAS-STING pathway that can be accentuated further with radiation treatment.

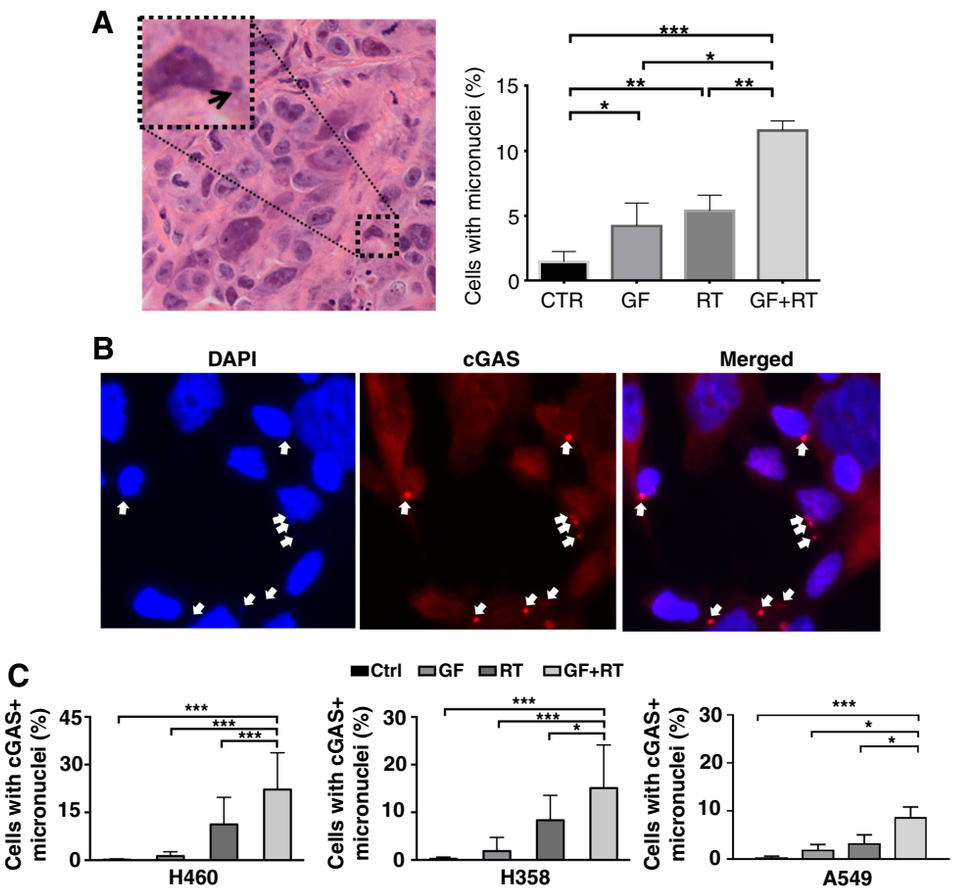

Figure 5.
CCi induces MN and activates cGAS. **A,** Representative H&E staining of the H358 tumor tissue showing regions of MN positive cells (left), and the quantification were shown in the right. **B,** Representative IF images of DAPI (blue) and cGAS (red) after treatment (t+48h) *in vitro* (40X magnification). **C,** Quantification of the percentage of cGAS-positive MN (cGAS+) cells from Ctrl, GF (15 μmol/L), radiation treatment (RT) (6 Gy), and GF+radiation treatment groups in H460, H358, and A549. Data were shown as average value ± SD calculated from three independent experiments (one-way ANOVA; *, $P < 0.05$; **, $P < 0.01$; ***, $P < 0.001$).

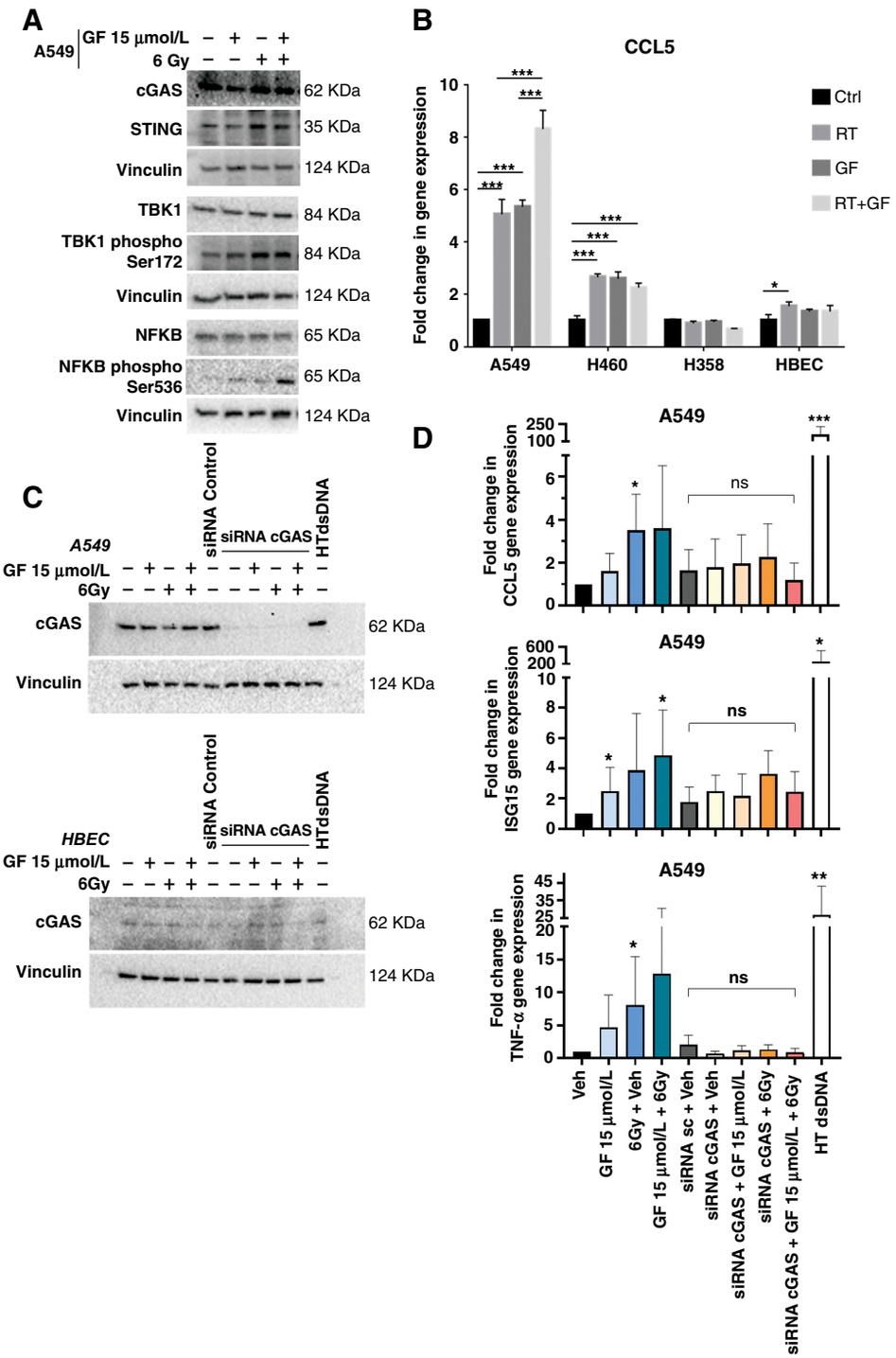

Figure 6.

The cGAS-STING pathway is activated after GF/radiation treatment (RT). **A,** Western blot analysis of cGAS, STING, TBK1, TBK1 phospho-Ser172, NFκB, NFκB phospho-Ser536, and Vinculin (loading control) protein expression in A549 after 15 µmol/L GF and/or 6 Gy radiation treatment. **B,** *CCL5* mRNA expression levels were measured by qPCR after different treatments *in vitro*. **C,** Western blot for cGAS and Vinculin (loading control) protein expression in A549 and HBEC without (Vehicle DMSO) or with 15 µmol/L GF and/or 6 Gy radiation treatment *in vitro*, and with or without siRNA against cGAS. HTdsDNA single treatment (24 hours) was used as positive control of cGAS-STING downstream pathway activation and target gene induction. **D,** *CCL5*, *ISG15*, *TNF-α* mRNA expression levels [reported against control Vehicle (Veh) condition] were measured by qPCR after treatments *in vitro* with or without siRNA against cGAS in A549. Data were shown as average value ± SD calculated from at least three independent experiments (*t* test/one-way ANOVA; ns, $P > 0.05$; *, $P < 0.05$; **, $P < 0.01$; ***, $P < 0.001$ compared with Veh condition, unless bracket showing against siRNA control).

Discussion

Tumor radioresistance is a major cause of failure in locally advanced NSCLC treatment. The development of drugs that can enhance the sensitivity of tumor cells to radiation is of great importance to improve the outcomes of NSCLC therapy, particularly for *KRAS*-mutant cases that have poor outcomes. CA in cancer cells can be caused by radiation treatment, and cancer cells have developed strategies to cluster extra-centrosomes to form pseudobipolar spindles for successful mitosis. In this study, we showed that GF radiosensitized NSCLC cells but not noncancer HBEC cells. GF can promote CCi, and genetic CCi with knockdown of the CC protein HSET also decreased cell viability of NSCLC cells to radiation treatment. GF treatment also induced the generation of MN, activating the cGAS-STING pathway, and increased the gene expression of downstream targets in NSCLC cells. Interestingly, further increase in the level of certain cGAS-STING target genes after combined radiation treatment and GF treatment were seen in the most radioresistant of the cell lines, A549. Our data suggest that CCi can radiosensitize NSCLC and that combination of CCi, radiation treatment, and immunotherapy is a potentially promising cancer treatment strategy that should be tested in NSCLC.

GF is an oral drug, inhibiting fungal cell mitosis, largely used in humans for the treatment of tinea capitis, as well as skin and nail dermatophytosis (12). GF has been shown to be able to alter cell cycle, to affect the stability of mitotic spindle, to inhibit cell proliferation, and induce apoptosis (9–11, 13, 14, 30). Many previous studies have shown that treatment with GF alone has antitumor activity (8, 9, 11, 13, 14, 30). In this study, we found that when combined with radiation treatment, GF significantly radiosensitized NSCLC cells, but not normal cells. Similar effects of CCi in cancer selective radiosensitization have also been reported in breast cancer cell lines *in vitro* recently (31). Therefore, all these results support further testing of CCi in radiotherapy in the future.

The cGAS-STING pathway plays an essential role in antitumor immune response. cGAMP synthase (cGAS) can detect cytosolic DNA fragments and generate the second messenger cGAMP, which activates the adaptor STING and downstream innate immune responses (32). MN are indicators of DNA damage, and cGAS localizes to MN arising from genomic instability in mouse and human cancer cells (29, 33). In our study, we presented the novel finding that GF and radiation treatment increased MN formation, over either treatment alone, resulting in more cGAS localization to MN. Interestingly, the most intrinsically radioresistant NSCLC cell line in our study, A549, showed the largest increase in the gene expression of the cGAS downstream targets with the combination GF+radiation treatment. Moreover, this was cGAS dependent as shown by cGAS knockdown experiments. The mechanism and significance of this finding could potentially lead to future novel therapeutic option especially in cases of radiation resistance and deserves further study to allow selective enhancement of the cGAS-STING pathway with immunotherapy.

Conclusions

Cancer cells frequently have amplified centrosomes and have developed strategies to cluster those extra-centrosomes to divide successfully. Here, we evaluated whether CCi can sensitize lung cancer cells (NSCLCs) to radiation treatment. We used pharmacologic and genetic methods to inhibit CC in lung cancer cells *in vitro* and *in vivo*. We demonstrated that CCi can selectively inhibit cancer cell proliferation, promote cell death, and lead to radiosensitization. Finally, CCi and radiation treatment resulted in increased MN and activation of the cGAS-STING pathway, which can potentially promote innate immunity. These characteristics may serve as a novel strategy to concurrently increase radiation response and antitumor immunity in locally advanced NSCLC.

Authors' Disclosures

C.L. Hann reports grants from AbbVie and Bristol Myers Squibb; grants and personal fees from Amgen and AstraZeneca; and personal fees from Genentech, Janssen, and Puma Biosciences during the conduct of the study. A. Holland reports grants and personal fees from Repare Inc and personal fees from Vibliome outside the submitted work. P.T. Tran reports personal fees from RefleXion Medical, Janssen, Bayer, AstraZeneca, and Natsar Pharmaceuticals during the conduct of the study. P.T. Tran has a patent for 9114158 issued to Natsar Pharmaceuticals with royalties paid from Natsar Pharmaceuticals. Other authors have declared that no conflict of interest exists. A. Lafargue reports on behalf of the group grants from NIH, Department of Defense, Prostate Cancer Foundation, Uniting Against Lung Cancer, Johns Hopkins and Allegheny Health Network, Radiological Society of North America; other support from Anonymous donor during the conduct of the study. No disclosures were reported by the other authors.

Authors' Contributions

X. Wang: Data curation, formal analysis, validation, investigation, methodology, writing–original draft, writing–review and editing. **N. Raman:** Data curation, formal analysis, validation, investigation, methodology, writing–review and editing. **G. Lemtiri-Chlieh:** Data curation, formal analysis, validation, investigation, methodology, writing–review and editing. **J. Chang:** Resources, data curation, validation, methodology. **S. Jagtap:** Resources, data curation, validation, methodology. **D.D. Chowdhury:** Resources, data curation, validation, methodology. **M. Ballew:** Resources, validation. **F.A. Carrieri:** Resources, validation, methodology, writing–review and editing. **T. Nguyen:** Resources, validation, methodology. **K. Nugent:** Resources, validation. **T. Peck:** Resources, validation. **M.S. Levine:** Resources, validation, methodology. **A. Chan:** Resources, methodology. **C. Lam:** Resources, validation. **R. Malek:** Resources, validation. **T. Hoang:** Resources, validation. **R. Phillips:** Resources, validation, writing–review and editing. **Z. Cheng:** Resources, validation. **K. Taparra:** Validation, writing–review and editing. **N. Connis:** Validation, writing–review and editing. **C.L. Hann:** Validation, writing–review and editing. **A. Holland:** Conceptualization, resources, supervision, investigation, methodology, writing–review and editing. **P.T. Tran:** Conceptualization, supervision, funding acquisition, validation, investigation, visualization, methodology, writing–original draft, project administration, writing–review and editing. **A. Lafargue:** Supervision, validation, investigation, visualization, writing–original draft, project administration, writing–review and editing. **H. Wang:** Conceptualization, data curation, formal analysis, supervision, funding acquisition, validation, investigation, visualization, methodology, writing–original draft, project administration, writing–review and editing.

Acknowledgments

P.T. Tran was funded by an anonymous donor, PCF-Movember Foundation-Distinguished Gentlemen's Ride-Prostate Cancer Foundation and the NIH/NCI (U01CA212007, U01CA231776 and U54CA273956) and DoD (W81XWH-21-1-0296). H. Wang is funded by a Uniting Against Lung Cancer Young Investigator Award and Johns Hopkins and Allegheny Health Network Award. A. Lafargue is funded by the DoD (W81XWH-18-1-0435). R. Malek is funded by the Prostate Cancer Foundation (PCF). R. Phillips is funded by the Radiological Society of North America. K. Taparra is funded by the NIH (F31CA189588).

The authors would like to acknowledge the SKCCC Experimental Irradiators Core at JHU (Esteban Velarde, M.S.), the Irradiation Core at UMB-DTRS (Kevin Byrne, M.S.), the Tissue Services Facility, and the Animal facility of the JHU-SKCCC for their support in this project.

The publication costs of this article were defrayed in part by the payment of publication fees. Therefore, and solely to indicate this fact, this article is hereby marked "advertisement" in accordance with 18 USC section 1734.

Note

Supplementary data for this article are available at Molecular Cancer Therapeutics Online (http://mct.aacrjournals.org/).

Received March 22, 2022; revised October 28, 2022; accepted January 31, 2023; published first February 7, 2023.

References

1. Siegel RL, Miller KD, Jemal A. Cancer statistics, 2017. CA Cancer J Clin 2017;67:7–30.
2. Siegel RL, Miller KD, Fuchs HE, Jemal A. Cancer statistics, 2022. CA Cancer J Clin 2022;72:7–33.
3. Tabchi S, Kassouf E, Rassy EE, Kourie HR, Martin J, Campeau M-P, et al. Management of stage III non-small cell lung cancer. Semin Oncol 2017;44:163–77.
4. Antonia SJ, Villegas A, Daniel D, Vicente D, Murakami S, Hui R, et al. Durvalumab after chemoradiotherapy in stage III non-small-cell lung cancer. N Engl J Med 2017;377:1919–29.
5. Cosenza MR, Cazzola A, Rossberg A, Schieber NL, Konotop G, Bausch E, et al. Asymmetric centriole numbers at spindle poles cause chromosome missegregation in cancer. Cell Rep 2017;20:1906–20.
6. Sato N, Mizumoto K, Nakamura M, Tanaka M. Radiation-induced centrosome overduplication and multiple mitotic spindles in human tumor cells. Exp Cell Res 2000;255:321–6.
7. Kwon M, Godinho SA, Chandhok NS, Ganem NJ, Azioune A, Thery M, et al. Mechanisms to suppress multipolar divisions in cancer cells with extra centrosomes. Genes Dev 2008;22:2189–203.
8. Kim Y, Alpmann P, Blaum-Feder S, Krämer S, Endo T, Lu D, et al. *In vivo* efficacy of griseofulvin against multiple myeloma. Leuk Res 2011;35:1070–3.
9. Rathinasamy K, Jindal B, Asthana J, Singh P, Balaji PV, Panda D. Griseofulvin stabilizes microtubule dynamics, activates p53 and inhibits the proliferation of MCF-7 cells synergistically with vinblastine. BMC Cancer 2010;10:213.
10. Panda D, Rathinasamy K, Santra MK, Wilson L. Kinetic suppression of microtubule dynamic instability by griseofulvin: implications for its possible use in the treatment of cancer. Proc Natl Acad Sci U S A 2005;102:9878–83.
11. Ho YS, Duh JS, Jeng JH, Wang YJ, Liang YC, Lin CH, et al. Griseofulvin potentiates antitumorigenesis effects of nocodazole through induction of apoptosis and G2/M cell cycle arrest in human colorectal cancer cells. Int J Cancer 2001;91:393–401.
12. De Carli L, Larizza L. Griseofulvin. Mutat Res 1988;195:91–126.
13. Raab MS, Breitkreutz I, Anderhub S, Rønnest MH, Leber B, Larsen TO, et al. GF-15, a novel inhibitor of centrosomal clustering, suppresses tumor cell growth *in vitro* and *in vivo*. Cancer Res 2012;72:5374–85.
14. Rebacz B, Larsen TO, Clausen MH, Rønnest MH, Löffler H, Ho AD, et al. Identification of griseofulvin as an inhibitor of centrosomal clustering in a phenotype-based screen. Cancer Res 2007;67:6342–50.
15. Madhav A, Andres A, Duong F, Mishra R, Haldar S, Liu Z, et al. Antagonizing CD105 enhances radiation sensitivity in prostate cancer. Oncogene 2018;37:4385–97.
16. Lu S, Ke Y, Wu C, Zhong Y, Xie C, Zhou Y, et al. Radiosensitization of clioquinol and zinc in human cancer cell lines. BMC Cancer 2018;18:448.
17. Wang Q, Ma J, Lu Y, Zhang S, Huang J, Chen J, et al. CDK20 interacts with KEAP1 to activate NRF2 and promotes radiochemoresistance in lung cancer cells. Oncogene 2017;36:5321–30.
18. Bakhoum SF, Ngo B, Laughney AM, Cavallo J-A, Murphy CJ, Ly P, et al. Chromosomal instability drives metastasis through a cytosolic DNA response. Nature 2018;553:467–72.
19. Strober W. Trypan blue exclusion test of cell viability. Curr Protoc Immunol 2015;111:A3.B.1–A3.B.3.
20. Zeng J, Aziz K, Chettiar ST, Aftab BT, Armour M, Gajula R, et al. Hedgehog pathway inhibition radiosensitizes non-small cell lung cancers. Int J Radiat Oncol Biol Phys 2013;86:143–9.
21. Wong J, Armour E, Kazanzides P, Iordachita I, Tryggestad E, Deng H, et al. High-resolution, small animal radiation research platform with x-ray tomographic guidance capabilities. Int J Radiat Oncol Biol Phys 2008;71:1591–9.
22. Franken NAP, Rodermond HM, Stap J, Haveman J, van Bree C. Clonogenic assay of cells *in vitro*. Nat Protoc 2006;1:2315–9.
23. Taparra K, Wang H, Malek R, Lafargue A, Barbhuiya MA, Wang X, et al. O-GlcNAcylation is required for mutant KRAS-induced lung tumorigenesis. J Clin Invest 2018;128:4924–37.
24. Jung CK, Jung JH, Lee KY, Kang CS, Kim M, Ko YH, et al. Centrosome abnormalities in non-small cell lung cancer: correlations with DNA aneuploidy and expression of cell cycle regulatory proteins. Pathol Res Pract 2007;203:839–47.
25. Marteil G, Guerrero A, Vieira AF, de Almeida BP, Machado P, Mendonça S, et al. Over-elongation of centrioles in cancer promotes centriole amplification and chromosome missegregation. Nat Commun 2018;9:1258.
26. Jiang F, Caraway NP, Li R, Katz RL. RNA silencing of S-phase kinase-interacting protein 2 inhibits proliferation and centrosome amplification in lung cancer cells. Oncogene 2005;24:3409–18.
27. Holland AJ, Cleveland DW. Chromoanagenesis and cancer: mechanisms and consequences of localized, complex chromosomal rearrangements. Nat Med 2012;18:1630–8.
28. Müller WU, Nüsse M, Miller BM, Slavotinek A, Viaggi S, Streffer C. Micronuclei: a biological indicator of radiation damage. Mutat Res 1996;366:163–9.
29. Storozynsky Q, Hitt MM. The impact of radiation-induced DNA damage on cGAS-STING-Mediated immune responses to cancer. Int J Mol Sci 2020;21:8877.
30. Mauro V, Carette D, Pontier-Bres R, Dompierre J, Czerucka D, Segretain D, et al. The anti-mitotic drug griseofulvin induces apoptosis of human germ cell tumor cells through a connexin 43-dependent molecular mechanism. Apoptosis 2013;18:480–91.
31. Choe MH, Kim J, Ahn J, Hwang S-G, Oh JS, Kim J-S. Centrosome clustering is a tumor-selective target for the improvement of radiotherapy in breast cancer cells. Anticancer Res 2018;38:3393–400.
32. Chen Q, Sun L, Chen ZJ. Regulation and function of the cGAS-STING pathway of cytosolic DNA sensing. Nat Immunol 2016;17:1142–9.
33. Mackenzie KJ, Carroll P, Martin C-A, Murina O, Fluteau A, Simpson DJ, et al. cGAS surveillance of micronuclei links genome instability to innate immunity. Nature 2017;548:461–5.